Heat conduction in one-dimensional oscillator lattices using Nosé–Hoover chain thermostats

2006 J. Phys. A: Math. Gen. 39 11155

(http://iopscience.iop.org/0305-4470/39/36/003)

INSTITUTE OF PHYSICS PUBLISHING JOURNAL OF PHYSICS A: MATHEMATICAL AND GENERAL

J. Phys. A: Math. Gen. **39** (2006) 11155–11170 doi:10.1088/0305-4470/39/36/003

Heat conduction in one-dimensional oscillator lattices using Nosé–Hoover chain thermostats

M Romero-Bastida and J F Aguilar

Centro de Investigación en Polímeros, Marcos Achar Lobatón No. 2, Tepexpan, 55885 Acolman, Estado de México, Mexico

E-mail: rbm@xanum.uam.mx and jaguilar@cip.org

Received 3 February 2006, in final form 22 June 2006
Published 18 August 2006
Online at stacks.iop.org/JPhysA/39/11155

Abstract

In this work, we numerically study the dynamical evolution and heat transport properties of a system that consists of two time-reversible thermostats connected either by a one-dimensional Fermi–Pasta–Ulam or a Frenkel–Kontorova oscillator lattice, which are representative models of momentum-conserving and nonconserving systems, respectively. The thermostats were described by a chain of variables, Nosé–Hoover chains, which enhances the ergodicity of the thermostats in comparison to the Nosé–Hoover method. The time evolution of both lattices is not significantly altered by the dynamics of the thermostats. The temperature profile and heat flux of the Fermi–Pasta–Ulam model are more sensitive to the dynamics of the extended variables than those corresponding to the Frenkel–Kontorova model. Nevertheless we reproduce the scaling properties of the thermal conductivity with system size obtained by other authors.

PACS numbers: 44.10.+i, 05.45.−a, 05.60.−k, 05.70.Ln

1. Introduction

Heat conduction in low-dimensional systems has been attracting increasing attention since the last decade (see review [1] and references therein). Notwithstanding the results so far achieved, it is still an open question under what dynamical conditions will the heat conduction obey the Fourier law. Since it was proposed that exponential instability might be the necessary condition [2], Lepri *et al* [3] studied the thermal conductivity of the one-dimensional Fermi–Pasta–Ulam (FPU) model of anharmonic oscillators by coupling each side of the lattice to deterministic Nosé–Hoover thermostats [4, 5] at high and low temperatures. They found a power-law divergence of the thermal conductivity with system size, which implies that the Fourier heat law is not justified in the FPU model,

where the momentum is a conserved quantity. Further studies have clarified that the size-dependence of the thermal conductivity is different between momentum-conserving and nonconserving systems, since it converges, in the limit of large system size, for the Frenkel–Kontorova (FK) model, where momentum is not conserved due to the existence of a on-site potential [6].

We emphasize that the study of low-dimensional models can be important to understand the behaviour of more sophisticated systems. For example, it has recently been shown that the thermal conductivity of a single walled carbon nanotube with a small diameter did not converge to a finite value with an increasing tube length, but obeyed a power-law relation strikingly similar to that previously obtained for the FPU model [7]. On the other hand, the FK model has been widely used to model crystal dislocation, charged density waves, absorbed epitaxial monolayers, etc in condensed matter physics (see [8] an references therein).

It has been pointed out that the Nosé–Hoover thermostats employed as heat reservoirs in the aforementioned studies of one-dimensional systems are not sufficiently chaotic (ergodic) to yield the canonical distribution from a single initial condition [9]. This observation has been invoked to argue the necessity to employ different thermostating schemes, such as homogeneous non-equilibrium molecular dynamics methods [10] or the Langevin model of heat reservoirs [11]. However, since the previously mentioned results for the FPU model are also obtained when stochastic heat reservoirs are employed [12], it seems that the thermal behaviour of the FPU and other one-dimensional models seems to be independent of the non-ergodicity of the Nosé–Hoover thermostats [1]. So it remains a problem to determine under which conditions is the macroscopic behaviour of a given thermostated system independent of the thermostat details. To address this problem we have to make a systematic study of the influence of the dynamical properties of the thermal reservoirs on the energy distribution in the lattice models herein studied. This entails the use of different deterministic thermostat models to asses which of their characteristics are relevant to the thermal properties of the studied lattice.

Among the large variety of generalizations of the original Nosé–Hoover thermostat (see review [13] and references therein) we have chosen a scheme, known as the Nosé–Hoover chain (NHC) method, that has become rather popular [14]. The method, originally proposed by Martyna *et al* [15] introduces a chain of Nosé–Hoover-type thermostats that successively thermostat each other, thus leading to trajectories that are sufficiently ergodic to ensure that all momenta have a Gaussian distribution. Although there has been a discussion about the proper statistical foundation for this method [16, 17], it is worth stressing that the NHC equations can be recast in a form [18] in which they are amenable to be treated by an alternative formulation [19] to the original (and very controversial) one [20]. It is also interesting to observe that, although the NHC method has been employed to study heat conduction in lattices with a Morse on-site potential [21], there has been no systematic comparison of the results of this new method with those provided by the conventional NH method.

In this paper we propose to make an assessment of the results of the NH and NHC methods applied to the problem of heat conduction in one-dimensional lattices to investigate why the non-ergodicity of the Nosé–Hoover thermostats apparently has no influence on the physical results so far reported in the literature. Furthermore, since the thermal conductivity is different in momentum conserving and non-conserving systems, as already remarked, we will take the FPU model and FK models as representative examples of the former and the latter type of systems. As we shall see, the type of potential that defines each particular model determines the influence of the thermostat dynamics on the thermal properties of the lattice.

2. The models

The Hamiltonian of the FPU model of N coupled nonlinear oscillators with nearest-neighbour interactions can be written, in terms of dimensionless variables, as

$$H = \sum_{i=0}^{N} \left[\frac{p_i^2}{2m_i} + \frac{1}{2}(x_{i+1} - x_i)^2 + \frac{1}{4}\beta(x_{i+1} - x_i)^4 \right], \tag{1}$$

where $\{x_i\}$ are the relative positions and $\{p_i\}$ the momenta. A value of $\beta = 0.1$ was employed in the computation of all the numerical results hereafter reported.

The FPU model presented above is a representative lattice without on-site potential and with momentum conservation. The FK model, on the other hand, is a representative of a general one-dimensional lattice with an on-site potential and without momentum conservation. The Hamiltonian of the standard FK model is

$$H = \sum_{i=0}^{N} \left[\frac{p_i^2}{2m_i} + \frac{1}{2}(x_{i+1} - x_i)^2 - \frac{K}{(2\pi)^2}\cos(2\pi[x_i + \mathrm{i}\mu]) \right], \tag{2}$$

where K is the strength of the external potential and μ is the *winding number*, which can be written in terms of the equilibrium distance a of the oscillators and the period b of the external potential before scaling as $\mu \equiv a/b$ [6]. In this work, we employed $\mu = 1/3$ and $K = 5$. For both models a mass of $m_i = 1$ is taken for all oscillators and fixed boundary conditions are assumed ($x_0 = x_{N+1} = 0$).

The previously defined Hamiltonians can be written in the general form

$$H = \sum_{i=0}^{N} \left[\frac{p_i^2}{2m_i} + V(x_{i+1} - x_i) + U(x_i) \right]. \tag{3}$$

Here $V(x_{i+1} - x_i)$ stands for the interaction potential of the nearest-neighbour oscillators and $U(x_i)$ is the periodic on-site potential. It is clear that if $U(x_i)$ vanishes and $V(x_{i+1} - x_i)$ takes the quadratic (harmonic) plus quartic form, equation (3) becomes the FPU model, and if the former potential takes the periodic form whereas the latter takes the harmonic form then the FK model (2) is obtained. By changing the form of $V(x_{i+1} - x_i)$ and $U(x_i)$ we obtain different thermal conductive behaviours.

3. Thermostat implementation

3.1. Nosé–Hoover method

The equations of motion for the standard NH method can be written as

$$\begin{aligned}
\dot{x}_i &= \frac{p_i}{m_i} \\
\dot{p}_i &= f_i - f_{i+1} - \frac{p_{\eta_i}}{Q_i} p_i (\delta_{i,1} + \delta_{i,N}) \\
\dot{\eta}_i &= \frac{p_{\eta_i}}{Q_i} (\delta_{i,1} + \delta_{i,N}) \\
\dot{p}_{\eta_i} &= \left\{ \frac{p_i^2}{m_i} - (T_+ \delta_{i,1} + T_- \delta_{i,N}) \right\} (\delta_{i,1} + \delta_{i,N}),
\end{aligned} \tag{4}$$

where $f_i \equiv -V'(x_{i+1} - x_i) - U'(x_i)$ is the force on each oscillator due to the potential, either of the FPU or FK type, and δ is the Kronecker symbol. Note that the boundary oscillators ($i = 1, N$) interact with two heat reservoirs operating at temperatures T_+ and T_-, respectively

(without loss of generality we assume that $T_+ > T_-$), in order to induce a heat flux through the lattice. The action of these thermostats is microscopically modelled by the set of extended variables $\{\eta_1, p_{\eta_1}, \eta_N, p_{\eta_N}\}$. The parameter Q_i, which can be considered as the 'mass' of each thermostat, determines the time scale on which the thermostats evolve and takes the form

$$Q_i = (T_+\delta_{i,1} + T_-\delta_{i,N})\Theta^2,$$

being Θ the thermostat response time [9]. The above prescriptions imply that the kinetic energy of the boundary oscillators fluctuates around the imposed average value, thus simulating a 'canonical' dynamics. The variables η_1 and η_N in (4) are decoupled from the dynamics and are strictly not necessary, but are given explicitly in order to compare with the NHC method. Indeed, if we define the thermodynamic friction coefficients as $\zeta_i \equiv \dot{\eta}_i$, we can recast equations (4) in the usual form encountered in this type of studies [1, 9].

The Nosé–Hoover thermostats were proposed as an extension of molecular dynamics methods to physical situations in which the total energy of the system is not constant, such as those corresponding to the NVT and NPT statistical ensembles [4, 5]. However, despite their widespread use, for small systems, such as an harmonic oscillator with a dynamics constrained by the condition of constant temperature, it has been shown that the resulting phase-space trajectories are incapable of reproducing the correct phase-space probability density function [5]. Since a single oscillator at each lattice end is thermostated by means of the NH method, as already explained, it is expected that the aforementioned lack of ergodicity of the boundary oscillators will somehow influence the thermal behaviour of the lattice. Then it would also be reasonable to believe that the results for heat conduction obtained by employing the NH thermostats would be somewhat modified if a different thermostating scheme is adopted.

3.2. *Nosé–Hoover chain method*

In [15] it was proposed to modify the NH method by including a series of thermostats coupled in such a way that the fluctuations of the first one are controlled by a second thermostat, its fluctuations being controlled by a third one, and so on, to form a chain of M thermostats. This set is named *Nosé–Hoover chain*. It has been explicitly demonstrated that, by employing this methodology, it is indeed possible to reproduce the phase-space probability density functions corresponding to various statistical ensembles [22].

The implementation of the NHC methodology to the heat conduction problem is straightforward, and the complete set of equations for the NHC method can be written as

$$\begin{aligned}
\dot{x}_i &= \frac{p_i}{m_i} \\
\dot{p}_i &= f_i - f_{i+1} - \frac{p_{\eta_{i,1}}}{Q_{\eta_{i,1}}} p_i(\delta_{i,1} + \delta_{i,N}) \\
\dot{\eta}_{i,\alpha} &= \frac{p_{\eta_{i,\alpha}}}{Q_{\eta_{i,\alpha}}}(\delta_{i,1} + \delta_{i,N}) \\
\dot{p}_{\eta_{i,1}} &= \left\{\left[\frac{p_i^2}{m_i} - (T_+\delta_{i,1} + T_-\delta_{i,N})\right] - p_{\eta_{i,1}}\frac{p_{\eta_{i,2}}}{Q_{\eta_{i,2}}}\right\}(\delta_{i,1} + \delta_{i,N}) \\
\dot{p}_{\eta_{i,\alpha}} &= \left\{\left[\frac{p_{\eta_{i,\alpha-1}}^2}{Q_{\eta_{i,\alpha-1}}} - (T_+\delta_{i,1} + T_-\delta_{i,N})\right] - p_{\eta_{i,\alpha}}\frac{p_{\eta_{i,\alpha+1}}}{Q_{\eta_{i,\alpha+1}}}\right\}(\delta_{i,1} + \delta_{i,N}) \\
\dot{p}_{\eta_{i,M}} &= \left\{\frac{p_{\eta_{i,M-1}}^2}{Q_{\eta_{i,M-1}}} - (T_+\delta_{i,1} + T_-\delta_{i,N})\right\}(\delta_{i,1} + \delta_{i,N}),
\end{aligned} \tag{5}$$

where a chain of M thermostats has been coupled to each boundary oscillator, as already explained. We take $Q_{\eta_{i,\alpha}} \equiv Q_i \ \forall \alpha$, which means that each αth element of the NH chain

of each boundary oscillator ($i = 1, N$) has the same value of the parameter Q_i originally employed in the NH method. This choice is not a limitation since small variations of particular values of the thermostat mass are not critical [5] (see the next section for further details on this particular issue). A point $\mathbf{\Gamma}(t)$ in the extended phase space is thus defined by

$$\mathbf{\Gamma}(t) = \left\{x_1, \ldots, x_N, p_1, \ldots, p_N; \{\eta_{1,\alpha}\}_{\alpha=1}^{M}, \{p_{\eta_{1,\alpha}}\}_{\alpha=1}^{M}, \{\eta_{N,\alpha}\}_{\alpha=1}^{M}, \{p_{\eta_{N,\alpha}}\}_{\alpha=1}^{M}\right\}.$$

Since each boundary oscillator is coupled to M extended variables, the NHC method increases the size of the phase space by the inclusion of the extended chain variables and thus helps make the system ergodic. Thus it can be expected that the dynamics of each boundary oscillator will be sufficiently chaotic to yield the canonical distribution consistent with the imposed temperature. In the next section, we will explore if this is indeed the case.

4. Phase-space dynamics

The equations of motion for both the NH and NHC methods corresponding to the FPU and FK models, although non-Hamiltonian in nature, are left invariant under time reversal composed with the change $p_i \to -p_i$. Thus they were numerically integrated by means of a explicit time-reversible integrator which preserves the structure of the extended phase space [23] and enabled us to employ a rather large integration step of 0.05 in all of our simulations. The values of N were taken between 32 and 512 (except for the computation of the thermal conductivity of the FPU model, for which we employed values up to $N = 16\,384$). In order to compare with previously published results [3, 6, 24] we take the value of the thermostat response time as $\Theta = 1$. As initial conditions we choose the equilibrium value of the oscillators displacements, i.e. $x_i(0) = 0\ \forall\ i$. The momenta $\{p_i(0)\}$ were taken randomly. Given this initial setting we proceed first to characterize the dynamics of the system, and then to investigate the influence of the NHC thermostats on the dynamics of the boundary oscillators and on the long-time behaviour of the lattice.

The maximum Lyapunov exponent (LE) gives a measure of the degree of chaos present in a dynamical system. In general, the more chaotic the dynamics of a system, the more quickly it fills the phase space. It is therefore important to study this quantity to corroborate if the Nosé–Hoover dynamics fills the accessible phase space for some reasonable values of the NHC length M. The calculation of the LE is based on dynamics cast in the generic form

$$\dot{\mathbf{\Gamma}}(t) = \mathbf{G}(\mathbf{\Gamma}),$$

where $\mathbf{\Gamma}(t)$ refers to a point in the extended phase space, as explained in the previous section. In the method used to calculate the exponents, two nearby trajectories are integrated for a small time interval τ and the distance between them monitored. The initial separation is determined by

$$\mathbf{\Gamma}'(0) = \mathbf{\Gamma}(0) + \delta\mathbf{\Gamma}(0),$$

where $\delta\mathbf{\Gamma}(0)$ is a vector such that $|\delta\mathbf{\Gamma}(0)| = \epsilon$, where $|\cdots|$ denotes the Euclidean norm. After an interval τ the norm $|\delta\mathbf{\Gamma}(\tau)|$ is computed and saved. The vector $\delta\mathbf{\Gamma}(\tau)$ is then renormalized to ϵ and the process is repeated N_τ times. The LE is calculated from

$$\lambda_{\max} = \frac{1}{N_\tau}\sum_{i=1}^{N_\tau} \ln\left|\frac{\delta\mathbf{\Gamma}_i(\tau)}{\epsilon}\right|. \tag{6}$$

In figure 1 the LE of both models is plotted as a function of M for two different values of the oscillator number N. The value $M = 0$ corresponds to the standard NH algorithm, whereas $M \geqslant 2$ corresponds to the NHC algorithm. The values of the employed temperature gradients

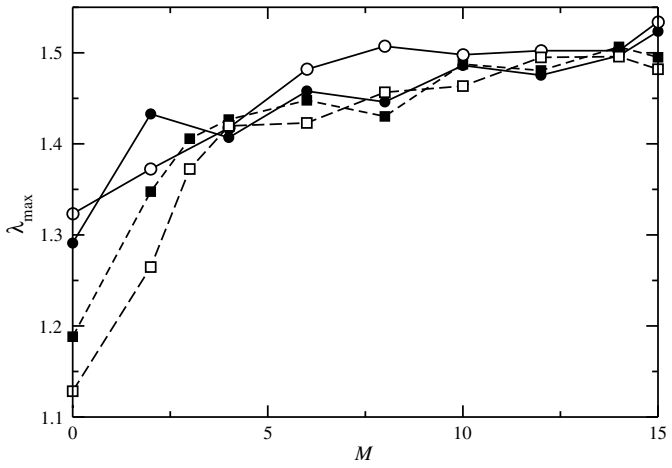

Figure 1. LE, computed from equation (6), for FPU and FK lattices as a function of the NHC length M. Filled circles and filled squares are the results corresponding to the FPU and FK models for $N = 32$, whereas open circles and open squares are the results with $N = 64$. The temperature gradients applied to the FPU and FK lattices for both N values are $\Delta T = 128$ and $\Delta T = 0.1$ respectively. The maximum standard deviation is $\mathcal{O}(10^{-3})$ for all data points. In all cases depicted $\tau = 10\Delta t$ and $N_\tau = 600\,000$.

were taken in a range, specific for each model, in which the corresponding temperature profiles are N independent (see section 5). In both instances the LE becomes increasingly large with M, whereas for $M \geqslant 10$ the dependence of the LE with respect to M becomes less pronounced. It is also observed that, for $M < 10$, the value of the LE depends strongly on the model. On the other hand, for $M \geqslant 10$ the average value of the LE is almost the same for both studied models. Therefore we can consider that a value of $M = 10$ guarantees that the trajectory generated by the Nosé–Hoover chain dynamics is ergodic enough to be compatible with the expected statistical behaviour of the boundary oscillators.

The dependence of the LE on N for both models is also reported in figure 1. We observe that this dependence is more pronounced in the case of the FPU model, since the large variations in the LE value for $N = 32$ are smoothened out for $N = 64$. The detected increase of the LE value with N for the FPU model seems to be consistent with the logarithmic divergence, albeit very weak, of the LE with N already reported [25]; although further research, which is out of the scope of this paper, is needed to clarify this point. In contrast, for the FK model the dependence $\lambda_{max}(N)$ is rather weak. Nevertheless, for $M \geqslant 10$ the LE of both models has already attained an almost N independent value.

For the FPU model it has been argued that the time evolution, obtained by means of the standard NH method, of the two thermostats at each end of the lattice is not sufficiently random, since some periodic-like structures can be detected in the phase space corresponding to each boundary oscillator [9]. However, in the case of the NHC method we obtain a somewhat different result. As can be readily seen in figure 2, the phase-space trajectory approximately fills the accessible phase space in the relatively short time interval depicted (almost four orders of magnitude lower than the time span employed to obtain the stationary state, as will be seen on the next section). Asymptotically no trace of any periodic-like structures, as well as of pathological structures such as Hoover Holes [15], can be observed, whatsoever. Thus we can conclude that, for the NHC method, the oscillators at both ends of the lattice are indeed well-behaved thermostats from a dynamical point of view. The corresponding results for the

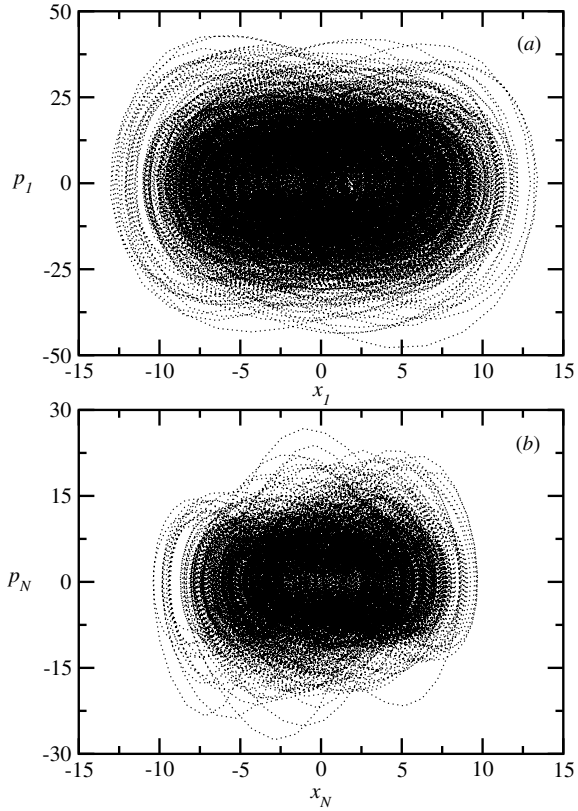

Figure 2. Phase space of the thermostated oscillators at each end of the FPU lattice, with (*a*) $T_+ = 152$ and (*b*) $T_- = 24$. Trajectory computed for an interval of 5.0×10^4 time steps. The NH chain length is $M = 10$ and the lattice size is $N = 32$.

FK model (not shown) are to a large extent the same as those displayed in figure 2, with only small differences due to the particular details of the model.

As previously mentioned, for the NH method the kinetic energy of the boundary oscillators fluctuates around the imposed average, thus their probability distribution functions are canonical. Now, for the NHC method it is essential to corroborate that this is indeed the case, since in another low-dimensional deterministic and periodic system such as the Lorentz gas it is known that slight modifications of the Nosé–Hoover thermostat lead to different dynamical and transport properties [26, 27]. By means of the analysis of the LE we have fixed the NHC length M, so the only free parameter left is the thermostat response time Θ taken provisionally as unity, as already mentioned. It is known that $\Theta \ll 1$ implies that there must be instantaneous response of the reservoir to the fluctuations of the kinetic energy of the boundary oscillators, thus imposing the constraint of constant kinetic energy which corresponds to the microcanonical ensemble; on the other hand, in the opposite limit $\Theta \gg 1$ the canonical distribution function is recovered [13]. However, the larger is Θ, the longer must last the simulations in order to have more reliable statistics. Hence an intermediate value in-between these two limiting cases would be the most appropriate choice.

In figure 3 we present the momentum distribution functions of the boundary oscillators corresponding to the FPU lattice for different values of the response time Θ. We do not discuss

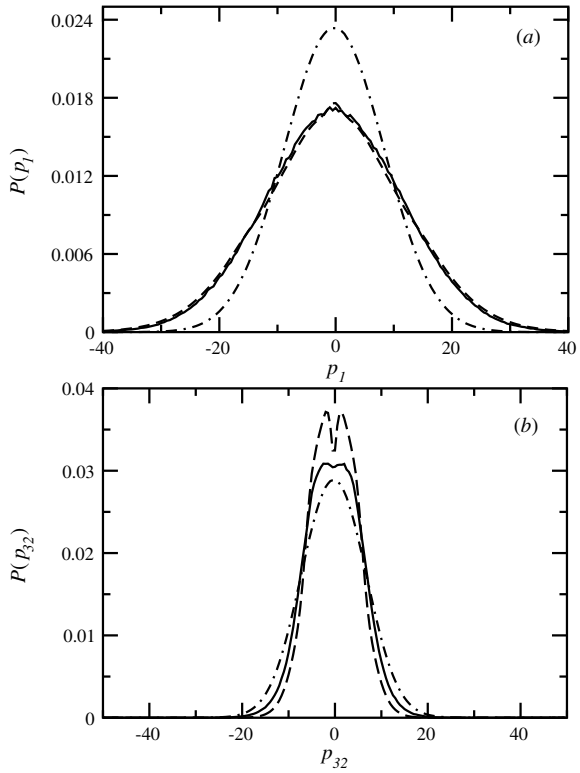

Figure 3. Momentum distribution functions obtained with a NHC length of $M = 10$ for (a) the first boundary oscillator thermostated at a temperature of $T_+ = 152$ and (b) the last oscillator thermostated at a temperature of $T_- = 24$ of a FPU lattice with $N = 32$. The response time of the boundary oscillators in both instances is $\Theta = 0.1$ (dashed curve), $\Theta = 1$ (solid curve) and $\Theta = 10$ (dot-dashed curve). Note the transition from a microcanonical-like to a canonical distribution under variation of Θ.

the probability densities for the associated position coordinates since the action of the thermal reservoir primarily concerns an exchange of energy related to the momenta. For the oscillator thermostated at the highest temperature $T_+ = 152$, the shape of the distribution function remains to a large extent Gaussian; only the height is affected by the Θ value, in agreement with the known results for the FPU model [1]. In contrast, for the oscillator thermostated at $T_- = 24$ it can be observed that, between the two limiting cases (microcanonical for $\Theta \ll 1$ and canonical for $\Theta \gg 1$) mentioned in the previous paragraph, there exists a superposition of the two corresponding distributions in the form of a *crater-like* distribution with a dip at the place of the maximum of the canonical distribution that is obtained for large Θ values. This result was first obtained for the periodic Lorentz gas [26], a system markedly different from those studied in the present work. By comparing the results in figures 3(a) and (b) for both temperature values we find that $\Theta = 1$ represents a reasonable compromise between the approach of the distribution function to the canonical form and numerical feasibility.

The corresponding results for the FK model are reported in figure 4. At variance with the results of the FPU we observe that the shape of the distribution functions always remains to a large extent Gaussian. No trace of the crater-like shape can be observed for all Θ values

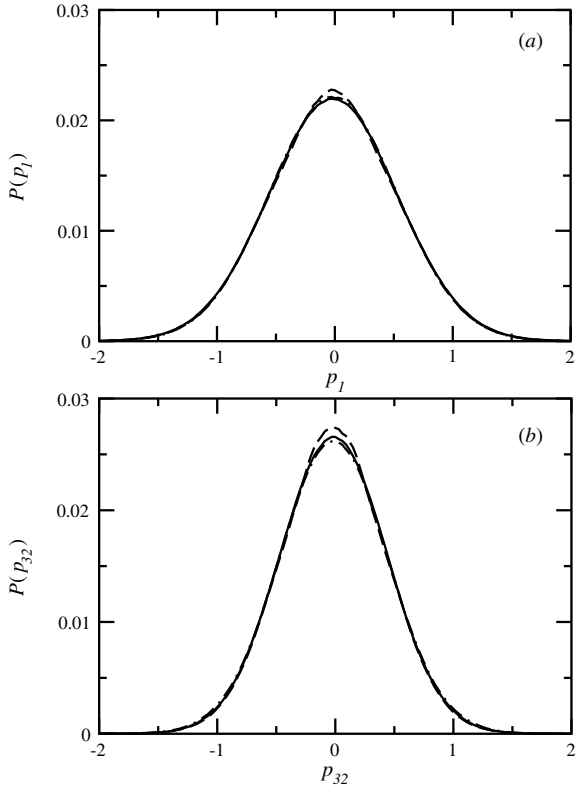

Figure 4. Momentum distribution function of (*a*) first boundary oscillator thermostated at $T_+ = 0.3$ and (*b*) last boundary oscillator thermostated at $T_- = 0.2$ for a FK lattice. Same N, M and Θ values, with same line symbols, as in figure 3.

employed. So, our results suggest that, for this model, the main features of the distribution functions of the boundary oscillators are almost unaltered by small variations of the thermostat response time. We believe that this result is due to the specific form of the on-site FK potential, although further research is needed to clarify this point. Thus, for the FK model we conclude that the choice $\Theta = 1$ is also an adequate value for the thermostat response time.

For the FPU model it is known that the existence of a nonlinear long-wavelength mode, which assists the energy transport, leads to the violation of the Fourier heat law in this one-dimensional system [9]. It is also known that the phonon–lattice interaction leads to a normal energy transport in the case of the FK model [6]. Our next objective is to investigate if the dynamics of the extended phase space has an influence in the above features of the studied lattices.

The time evolution, after a long transient time interval of 2×10^8 time steps, of the relative positions $\{x_i\}$ in a lattice with $N = 128$ oscillators and a NH chain length of $M = 10$ is plotted in figure 5(*a*). The grey-scale changes from black to white correspond to a change from minimum to maximum. This figure gives clear evidence of the nonlinear long-wavelength mode, which corresponds to the longest oscillation visible during the simulation interval. The regular energy transport along the FPU lattice leads to a long-time correlation between oscillators in the system [9]. This can be quantified by following the time evolution of

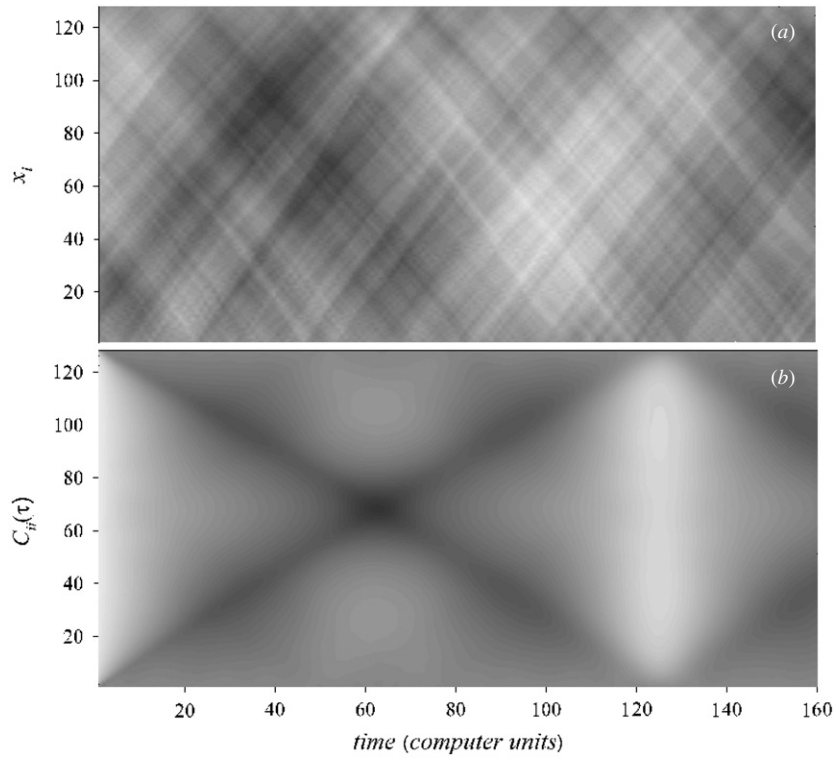

Figure 5. (*a*) Time evolution of the displacements and (*b*) time evolution of the normalized autocorrelation function of a FPU lattice with $N = 128$ oscillators and NHC length of $M = 10$.

the correlation function $C_{ij}(\tau) = \langle x_i(t)x_j(t+\tau)\rangle$, with $\langle\cdots\rangle$ denoting time average. The normalized autocorrelation function C_{ii} is shown in figure 5(*b*), in which the quasiperiodic correlations inside the chain are clearly visible. These correlations are produced by the aforementioned long wave-length mode which has a period proportional to N, as can be appreciated in that same figure. Since these last results are entirely consistent with those found employing the NH method, we conclude that the dynamical behaviour of the lattice is unaffected by the change in the thermostating mechanism afforded by the NH chain.

As already mentioned, the on-site potential in the FK model inhibits the long-wavelength mode present in the FPU model. A direct corroboration is afforded by the information presented in figure 6(*a*) for the time evolution of the relative positions $\{x_i\}$. At variance with the results of figure 5(*a*) for the FPU lattice, the long-wavelength mode is altogether absent in the case of the FK model. Furthermore, by following the time evolution of C_{ii}, the correlations inside the lattice gradually die out, as can be appreciated in figure 6(*b*).

Our results so far establish that the NHC method is more adequate than the standard NH method to model the thermostats which drive the system to the steady state. The influence of the extended variables is not appreciated in the dynamical behaviour of the lattice for both the FPU and FK models, which is mainly driven by the specific features of the respective potentials, as already known form previous studies. In the next section, we will investigate the influence, if any, of the extended variables in the energy transport properties for both models.

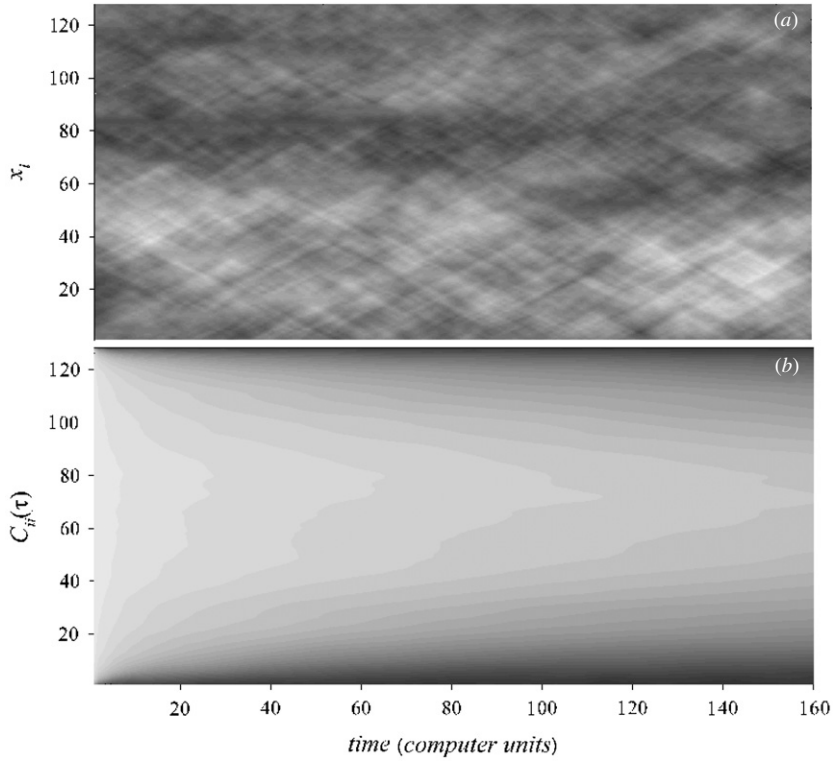

Figure 6. (*a*) Time evolution of the displacements and (*b*) time evolution of the normalized autocorrelation function of a FK lattice with $N = 128$ oscillators and NHC length of $M = 10$.

5. Temperature profile and heat flux

After a long transient time interval of 2×10^8 time steps, the system reaches a statistically stationary state, where each oscillator is in a local equilibrium at a certain kinetic temperature of $T_i = \langle p_i/m_i \rangle$. The non-equilibrium macrostate is characterized by a non-uniform temperature field along the lattice which converges to a well-defined shape. In figure 7, we present our results for the FPU model corresponding to the NH and NHC methods for a lattice size of $N = 128$. By comparing the results of both methods we can readily observe some differences. First, the singularities at both lattice ends are somewhat increased in the case of the NHC method. This boundary-resistance can be explained by the existence of quasi-conserved modes associated with the boundary oscillators [28]. The rigidity of these modes is thus enhanced by the more detailed microscopic dynamical description of the thermostats afforded by the NHC method. It is also known that these thermal resistance effects are a signature of the anomalous transport properties that are characteristic of this model [1]. Now, since the oscillators in the bulk are less affected by the microscopic details of the thermostats, we can infer that, as N increases, the thermal properties of the lattice will not be significantly altered by the NH chains that thermostat the boundary oscillators.

For the case of the FK model, the dependence of the temperature profile shape on the NH chain length is almost negligible, as can be seen in figure 8. Thus it is clear that the presence of the on-site potential, which is responsible of the normal heat conduction in the FK model [6],

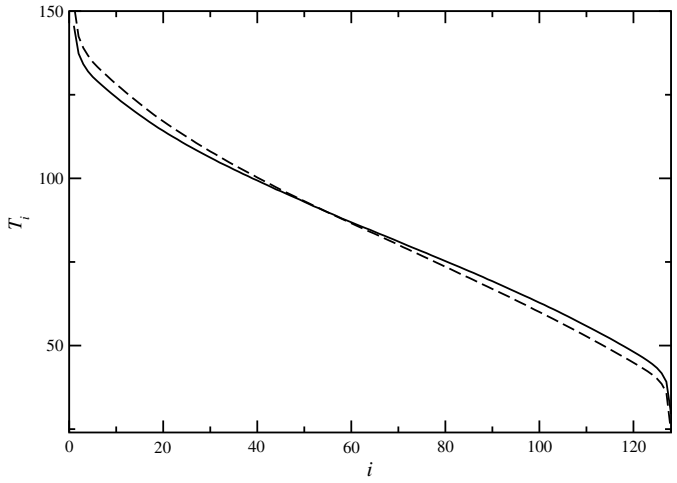

Figure 7. A temperature profile of the FPU lattice. The imposed temperatures are $T_+ = 152$ and $T_- = 24$, with an oscillator number of $N = 128$. Averages are carried over a time interval of $\approx 10^5$ time steps. The displayed results are for the NH (dashed line) and NHC (solid line) methods, with $M = 10$ in the latter case. The maximum standard deviation is $\mathcal{O}(10^{-2})$ for all data points.

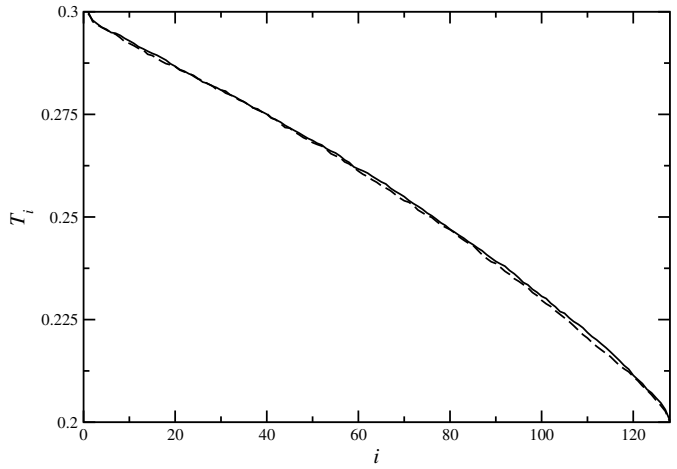

Figure 8. Temperature profile of the FK lattice. The imposed temperatures are $T_+ = 0.3$ and $T_- = 0.2$, with an oscillator number of $N = 128$. Results for the NH (dashed line) and NHC (solid line) methods, with $M = 10$ in the latter case. Same maximum standard deviation as in figure 7 for all data points.

makes the FK lattice incapable of sustaining the quasi-conserved modes present in the FPU lattice, a feature that also drastically diminishes the influence of the extended variables on the non-equilibrium macrostate. From these results it is clear that, so far, the differences between the NH and NHC methods can only be attributed to the type of potential and the dynamical details in each lattice model, and not to the differences in the microscopic description of the thermostats employed in both methods.

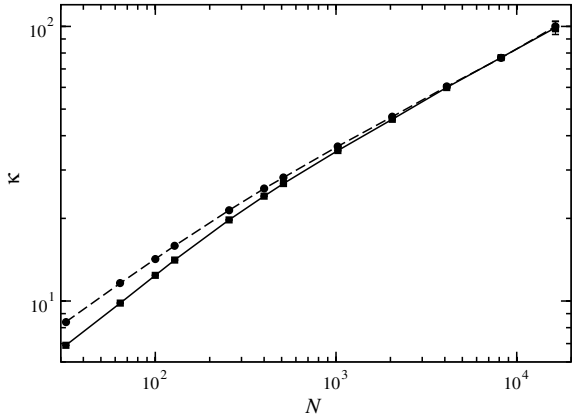

Figure 9. $\kappa(N)$ versus oscillator number N for the FPU lattice. Results for the NH (circles, dashed line) and NHC (squares, solid line) methods, with $M = 10$ in the latter case. $T_+ = 152$ and $T_- = 24$ in both cases. The lines are drawn to guide the eye. Statistical errors are displayed only when larger than the symbols' size.

The local heat flux $j(q,t) = \sum_i J_i \delta(q - q_i)$, where $q_i = x_i + \mathrm{i}\mu$, is implicitly defined by the continuity equation [6]. Thus the heat flux is defined as

$$J_i = \frac{p_i}{m_i} \frac{\partial V(x_{i+1} - x_i)}{\partial x_i}.$$

Numerically, the time average $J = \langle J_i(t) \rangle$ is independent of the index i for long enough time.

We now proceed to explore the influence of the thermostat description on the thermal conductivity of the FPU lattice. For a different particle number N, the corresponding temperature profiles scale as $T_i = T(i/N)$ (see figure 1 in [3]), which implies that the temperature gradient vanishes as N^{-1}. In figure 9, we have plotted the finite-length thermal conductivity $\kappa(N) = JN/\Delta T$ as a function of the oscillator number N computed with the NH and NHC methods. In both cases, it is clear that the conductivity diverges as $\kappa \propto N^\alpha$. However, we note that the finite-size effects are much more pronounced in the results corresponding to the NHC method than those of the conventional NH method. Indeed, the crossover in the dependence of the α exponent on N, first detected in [24] at $N = 250$ employing the NH method, is somewhat increased to $N = 1024$ for the case of the NHC method. To obtain information on the behaviour of the α exponent in the thermodynamic limit we have to discard data points that present a strong finite-size dependence, which can be readily identified, by means of the NHC method, as those corresponding to $N < 1000$. Our result for the NH method is $\alpha = 0.361 \pm 0.003$, in good agreement with the first published results [3, 24], whereas for the NHC method we obtain $\alpha = 0.372 \pm 0.003$, a value consistent both with latter simulation results, albeit obtained for a temperature gradient of $\Delta T = 16$, and with the predictions of self-consistent mode-coupling theory [29]. Both results are larger than the $\alpha = 1/3$ estimate obtained by a renormalization group calculation on the stochastic hydrodynamic equations of a 1D fluid [30]. Furthermore, we observe that, notwithstanding the large lattice sizes employed in the computation of α, its value, obtained by means of the NHC method, is systematically different than that computed with the conventional NH method. Further studies are needed to corroborate if this difference persists with different simulation conditions, such as larger system sizes and smaller temperature gradients.

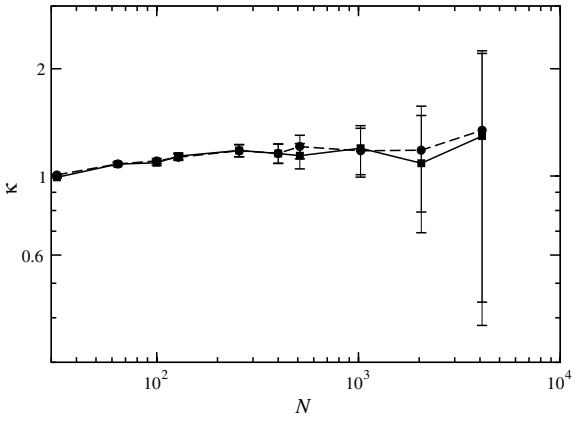

Figure 10. $\kappa(N)$ versus oscillator number N for the FK lattice. Results for the NH (circles, dashed line) and NHC (squares, solid line) methods, with $M = 10$ in the latter case. $T_+ = 0.3$ and $T_- = 0.2$ in both cases. The lines are drawn to guide the eye.

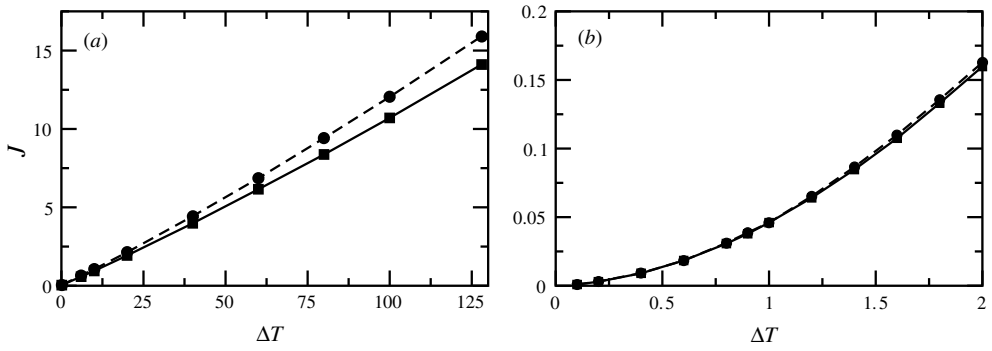

Figure 11. Average heat flux versus temperature gradient for (*a*) FPU and (*b*) FK lattices, both with $N = 128$ oscillators. Results for the NH (circles, dashed line) and NHC (squares, solid line) methods, with $M = 10$ in the latter case. The maximum standard deviations for the FPU and FK data are $\mathcal{O}(10^{-3})$ and $\mathcal{O}(10^{-5})$, respectively. The lines are drawn to guide the eye.

In the case of the FK lattice, the scaling of the finite-length conductivity $\kappa(N)$ with oscillator number N is almost independent of the employed method, either NH or NHC, as can be readily appreciated in figure 10. Only for a lattice length greater than 400 the thermal conductivity presents a weak size dependence which is nevertheless statistically not significant. The small value of the temperature gradient compared to the strength of the on-site potential guarantees that the scaling relation $T_i = T(i/N)$ is satisfied for the FK model (see figure 1 in [6]), which implies that the temperature gradient vanishes as N^{-1}, just as in the FPU model. Since the approximately constant value of $\kappa(N)$ for all N values implies that $1/J$ diverges with N, the thermal conductivity is finite and the Fourier heat law is justified.

Figure 11(*a*) shows the mean heat flux as a function of the temperature gradient ΔT for the FPU model. It is observed that, as the temperature difference increases, the averaged heat flux increases monotonically [31]. We again find a dependence of the result on the employed thermostat description. For the NHC method the value of the average heat flux diminishes with

respect to the corresponding value obtained from the NH method when both are computed at the same temperature difference.

For the FK model, the increase in the average heat flux with the temperature gradient has a parabolic-type shape, as can be seen in figure 11(*b*). This result is almost the same for both the NH and NHC methods. We again find that the on-site potential strongly diminishes the influence of the chosen dynamical description of the heat baths on the thermal behaviour of the lattice. We remark that our results for the FK model are rather different from those obtained recently for the ϕ^4 model [31]. For this model, which is described by the potentials $V(x) = \frac{1}{2}x^2$ and $U(x) = \frac{1}{2}x^2 + \frac{1}{4}x^4$, the average heat flux saturates at a certain value of the temperature gradient without any further increase. It has been argued that this peculiar behaviour of the ϕ^4 model is due to a combination of nonintegrability and lack of momentum conservation [31]. Now, although the temperature gradients that we employed for the FK model are much smaller than those employed in [31] for the ϕ^4 model for reasons already explained, nevertheless the behaviour of the average heat flux is markedly different from that of the ϕ^4 model, even though both models are nonintegrable and lack momentum conservation. Furthermore, the saturation of the average heat flux at a certain threshold value of ΔT_c has also been observed in a chain of coupled rotators ($V(x) = 1 - \cos(x)$ and $U(x) = 0$), which has no on-site potential and where momentum is conserved [11, 32]. From our results and the aforementioned comparisons we can conclude that the mechanism responsible of the saturation of the average heat flux beyond certain threshold temperature gradient value for the ϕ^4 model so far remains unexplained.

6. Conclusions

In this paper, we have applied the Nosé–Hoover chain method of extended variables to describe the microscopic dynamics of the time-reversible thermostats coupled to FPU and FK lattices. With this method the ergodicity of each thermostat is increased and the phase-space trajectory fills the accessible phase-space. Next we have shown that the long time evolution of both lattices is not significantly affected by the thermostat description. Our results also show that the temperature profile as well as the heat flux of the FPU lattice are indeed affected by the type of microscopic description employed in the thermostats, a behaviour that is not detected in the corresponding results for the FK lattice. In any case the corresponding scaling of the thermal conductivity with the system size, which is the physically relevant result, is only weakly affected by these differences for large enough lattices. Thus we have explained why, despite the non-ergodicity exhibited by the most frequently employed Nosé–Hoover thermostats, the results so far reported in the literature are consistent.

Furthermore, it is important to note that the insights gained in the study of these simplified models are useful to understand the behaviour of systems described by more sophisticated potentials. For example, the harmonic part of potential (1) can be considered as a second-order approximation, in a Taylor expansion, to the Tersoff potential usually employed in theoretical studies of carbon nanotubes [7]. This feature has indeed been invoked as the reason of the similitude in the behaviour of the thermal conductivity of these systems and that first observed in the FPU model [33]. On the other hand, the on-site potential of the FK model can be considered as a particular approximation to the many-body effects that are incorporated, by means of an on-site potential, in the embedded-atom method used to describe interactions in metals [34].

The reported results lead us to conclude that the presence of the on-site potential, which accounts for the finite thermal conductivity of the FK lattice, is also responsible of the negligible effect of the chain variables on the thermal behaviour of the FK model, although the precise

mechanism responsible of this behaviour remains hitherto unclear. Furthermore, considering the results of the present paper, it cannot be discarded that the FK lattice could exhibit a different thermal behaviour under the influence of another type of chain thermostat, such as that proposed in [35].

Acknowledgments

We want to thank M C Nuñez-Santiago for her help in the three-dimensional plots and for useful discussions. Financial support from Consejo Nacional de Ciencia y Tecnología (CONACyT) is also acknowledged. We thank the referees for helpful suggestions to improve this work.

References

[1] Lepri S, Livi R and Politi A 2003 *Phys. Rep.* **377** 1–80
[2] Casati G, Ford J, Vivaldi F and Visscher W M 1984 *Phys. Rev. Lett.* **52** 1861–4
[3] Lepri S, Livi R and Politi A 1997 *Phys. Rev. Lett.* **78** 1896–9
[4] Nosé S 1984 *J. Chem. Phys.* **81** 511–9
[5] Hoover W G 1985 *Phys. Rev.* A **31** 1695–1997
[6] Hu B, Li B and Zhao H 1998 *Phys. Rev.* E **57** 2992–95
[7] Murayama S 2002 *Phys.* B **323** 193–5
[8] Bak P 1982 *Rep. Prog. Phys.* **45** 587–629
[9] Fillipov A, Hu B, Li B and Zeltser A 1998 *J. Phys. A: Math. Gen.* **31** 7719–28
[10] Zhang F, Isbister D J and Evans D J 2000 *Phys. Rev.* E **61** 3541–6
[11] Gendelman O V and Savin A V 2000 *Phys. Rev. Lett.* **84** 2381–4
[12] Kaburaki H and Machida M 1993 *Phys. Lett.* A **181** 85–90
[13] Klages R 2003 *Preprint* nlin.CD/0309069
[14] Frenkel D and Smit B 2002 *Understanding Molecular Simulations: From Algorithms to Applications* 2nd edn (San Diego: Academic)
[15] Martyna G J, Klein M L and Tuckerman M E 1992 *J. Chem. Phys.* **97** 2635–43
[16] Ramshaw J D 2002 *Europhys. Lett.* **59** 319–23
[17] Sergi A 2005 *Preprint* cond-mat/0511343
[18] Sergi A and Ferrario M 2001 *Phys. Rev.* E **64** 056125-1, 9
[19] Sergi A 2003 *Phys. Rev.* E **67** 021101-1,7
[20] Tuckerman M E, Mundy C J and Martyna G J 1999 *Europhys. Lett.* **45** 149–53
[21] Terraneo M, Peyrard M and Casati G 2002 *Phys. Rev. Lett.* **88** 094302–1, 4
[22] Tuckerman M E, Liu Y, Ciccotti G and Martyna G J 2001 *J. Chem. Phys.* **115** 1678–702
[23] Martyna G J, Tuckerman M E, Tobias D J and Klein M L 1996 *Mol. Phys.* **87** 1117–54
[24] Lepri S, Livi R and Politi A 1998 *Phys.* D **119** 140–7
[25] Searles D J, Evans D J and Isbister D J 1997 *Phys.* D **240** 96–104
[26] Rateitschak K, Klages R and Hoover W G 2000 *J. Stat. Phys.* **101** 61–77
[27] Rateitschak K, Klages R and Nicolis G 2000 *J. Stat. Phys.* **99** 1339–64
[28] Alabiso C, Casartelli M and Marenzoni P 1995 *J. Stat. Phys.* **79** 451–71
[29] Lepri S, Livi R and Politi A 1998 *Europhys. Lett.* **43** 271–6
[30] Narayan O and Ramaswamy S 2002 *Phys. Rev. Lett.* **89** 200601-1, 4
[31] Ueda A and Takesue S 2005 *Preprint* cond-mat/0508619
[32] Giardiá C, Livi R, Politi A and Vassalli M 2000 *Phys. Rev. Lett.* **84** 2144–7
[33] Li B, Wang J, Wang L and Zhang G 2005 *Chaos* **15** 015121–1, 13
[34] Daw M S and Baskes M J 1983 *Phys. Rev. Lett.* **50** 1285–8
[35] Liu Y and Tuckerman M E 2000 *J. Chem. Phys.* **112** 1685–700